Received: 3 February 2025 | Revised: 25 August 2025 | Accepted: 30 October 2025

DOI: 10.1002/zamm.70288

ORIGINAL PAPER

Harnessing of potential Hall and Dufour Effects on MHD flow over a parabolically accelerated vertical plate

A. Selvaraj[1] | **M. Aruna**[2] | **S. Deepa**[3] | **S. Dilip Jose**[4] | **S. Sahaya Jude Dhas**[5] | **Mohammed T. Alotaibi**[6]

[1]Department of Mathematics, Vels Institute of Science, Technology and Advanced Studies, Chennai, Tamil Nadu, India

[2]Department of Mathematics, Tagore Institute of Engineering and Technology, Salem, Tamil Nadu, India

[3]Department of Mathematics, Vel Tech High Tech Dr.Rangarajan Dr.Sakunthala Engineering College, Chennai, Tamil Nadu, India

[4]Department of Mathematics, Periyar Maniammai Institute of Science & Technology (Deemed to be University), Thanjavur, Tamil Nadu, India

[5]Saveetha School of Engineering, Saveetha Institute of Medical and Technical Sciences, Saveetha University, Chennai, Tamil Nadu, India

[6]Department of Chemistry, Turabah University College, Taif University, P.O. Box 11099, Taif 21944, Saudi Arabia

Correspondence
A. Selvaraj, Department of Mathematics, Vels Institute of Science, Technology and Advanced Studies, Chennai, Tamil Nadu, India.
Email: aselvaraj_ind@yahoo.co.in

S. Sahaya Jude Dhas, Saveetha School of Engineering, Saveetha Institute of Medical and Technical Sciences, Saveetha University, Chennai, Tamil Nadu, India.
Email: judedhas@gmail.com

This research work investigates the Hall and Dufour Effects, as well as the impact of rotation, on magnetohydrodynamic flow over a parabolically accelerated vertical plate with uniform temperature and variable mass diffusion. In contrast to other studies that investigated these effects independently or under steady plate motion, this work evaluates their combined impact in a transient, parabolically accelerated condition in an entirely novel way. The precise nature of this impact is still not very clear despite relevant computations being made. Both the plate temperatures and the nearby concentration levels have increased consistently and uniformly. The dimensionless form was obtained by applying the Laplace transform. The Schmidt number, Ludwig Prandtl number, thermal Franz Grashof number, and mass Franz Grashof number were among the physical parameters that were assessed. For the profiles to be visually represented, these properties were included with the effects of velocity, temperature, and the number of species dissolved in the liquid. The liquid stream equation concepts are developed by implementing MATLAB software. Increased velocity measurements are the result of an increase in the thermal (or mass) Grashof number. A reversal of the trend has been observed in the Dufour and magnetic field characteristics. In the investigated settings, the temperature and concentration levels near the plate both steadily increase. This formulation provides a more thorough understanding of coupled electromagnetic–thermal–mass diffusion phenomena in electrically conducting fluids by integrating Hall currents, Dufour heat transfer, and rotational effects. It may find use in material processing, energy systems, and industrial cooling. Moreover, the current analysis illustrates the effects of Schmidt number variation and time-dependent concentration decay on the concentration boundary layer in MHD flows. This information is essential for optimizing processes where mass transfer under magnetic fields is a governing factor, such as metallurgical operations, chemical reactors, cooling systems, and biomedical transport.

© 2025 Wiley-VCH GmbH.

1 | INTRODUCTION

Magnetohydrodynamic (MHD) flow has attracted a lot of interest because of its applications in geophysical fluid dynamics, engineering, and astrophysics. The behaviour of electrically conducting fluids in a variety of physical environments is significantly impacted by phenomena like the Hall and Dufour effects, which occur in the presence of magnetic fields and thermal gradients, respectively. These effects are especially important in processes like cooling technologies, crystal growth, and plasma physics that involve the transfer of mass and heat in rotating systems. The quest to find a stable water source prompted the need to comprehend fluid dynamics. The consensus was that wells needed to be dug out and basic pumping equipment needed to be installed. The growing population further exacerbated the urgent need for fundamental knowledge and a fast solution for sewage disposal. Learning that water could be harnessed to generate electricity and move cargo was a huge exhilaration. Within urban areas, rivers naturally grew longer and wider as cities expanded. Particularly evident in the construction of "thermal energy stations, steel factories, gas turbines, and different aeroplane propulsion frameworks," among other applications, the modern era is entirely made up of ignition and reactor design. Important factors in the design of reactor and combustion systems include energy consumption, temperature, and heat transfer effects, material processing, and "heat and mass transfer effects." In the middle of the 1800s, the Navier-Stokes equations, which govern fluid flow, were thought to be too complicated to solve [1, 2].

With the advent of diverse corporations at the turn of the century, there was a need for scientific knowledge that could be applied to a wide range of fluids rather than equations that were specific to each fluid. As a result of this requirement, a number of novel ideas that have impacted fluid dynamics were developed. Selvaraj and Jothi [3] investigated how an intensity source affected radiation intake and MHD as a liquid moved through a penetrable material. Their focus is also seen as mass dispersion over an exponentially increasing vertical board with exponentially fluctuating temperature. The rotational effects of a parabolic stream through an accelerated isothermal vertical panel with fluctuating temperature and constant mass diffusion were investigated by Sindhu et al. [4]. The fluid dynamics of an unsteady MHD parabolic stream through an accelerated vertical panel with rotation in a permeable material was examined in another study by Gowri and Selvaraj [5]. Furthermore, the effects of revolution on a parabolic stream past an accelerated isothermal vertical panel with heat and mass diffusion were explored by Selvaraj et al. [6].

Jothi et al. [7] performed a thorough investigation of the effects of radiation absorption and MHD on fluid flow past a vertically accelerated panel with different temperatures and concentrations. Aruna et al. [8] demonstrated the Hall and magnetic effects on a stream that passes a parabolically accelerated vertical panel with fluctuating thermal conditions and constant mass diffusion when thermal radiation is present. The Hall and heat source effects of a stream passing a parabolically accelerated isothermal vertical panel in the presence of radiation and chemical reactions are examined by Lakshmikaanth et al. [9]. Jothi and Selvaraj's study [10] focused on examining the Dufour influence on the MHD stream through a vertical board that speeds up exponentially in a porous framework with varying mass and temperature dispersion. Additionally, in an environment of chemical reaction and Hall current, stream impacts of a parabolically propelled isothermal upward surface are explained by Lakshmikaanth et al. [11]. Jothi and Selvaraj [12] examine the effect of Dufour in a thin MHD stream passing through a penetrable material with an upward-slanted board that rapidly accelerates while taking different temperatures and mass dispersion into account. They also study the effects of Dufour and Hall on MHD flow through a vertical panel with variable mass diffusion and temperature and exponential acceleration.

Dufour and Hall effects on the MHD stream surrounding a vertically oriented panel experiencing exponential acceleration have been studied by Angela and Selvaraj [13], accounting for temperature and mass diffusion changes. The purpose of the study is to look into how stable fluid flux is in these circumstances. The effect of a continuous radial electric field on the MHD heat and fluid flux produced by a rotating disc was examined by Mustafa Turkyilmazoglu [14]. The study most likely examined how the liquid rotated when subjected to electric fields. Armstrong and Priyadarshini [15] investigated the skin friction properties of a panel with a parabolic profile that is extensively vertical. In addition to the impact of an attractive field, the analysis considered variations in temperature and mass dispersion. An investigation into convective heat and mass transfer in a magnetohydrodynamic setting between infinitely tall vertical panels, taking into account the influence of the Soret effect and Joule dissipation, was described by Reddy et al. [16]. The paper also offers a brief explanation of joule dissipation.

The impact of Dufour and Soret phenomena on continuous MHD flow over an inclined stretching sheet with heat generation and a magnetic field was investigated by Karim et al. [17]. In this study, the researchers shared their relevant findings, such that they examined the effects of radiation, Soret, Dufour, and other effects, as well as chemical reactions and a heat source, on the MHD flow of a dissipative fluid past a permeable plate. The study explores how the fluid behaves

as it passes through the permeable plate. In their study, Verma and Sharma [18] investigated the effects of Soret and Dufour impacts on heat and mass transfer, as well as MHD flux, over a sheet that can stretch exponentially. On the basis of this research, the researchers presented their conclusions. Ercan et al. [19] looked at the Hall effect on MHD and heat transfer with a constant electric domain. The focus of an investigation by Armstrong et al. [20] was the rotatory effects of an explanatory transition past an upward plate over a penetrable material with different temperatures and uniform mass distribution. Their decision in light of their examination was expressed by the expression's expansion. Based on their exploration, the experts presented their findings. In the framework of MHD, Seth et al. [21] researched the MHD free convection with rotational impact in a moving vertical plate. Muthucumaraswamy R. et al. [22] investigated the effects of the Hall impact on a vertically moving isothermal panel while taking temperature and mass diffusion changes in the presence of a rotating fluid into consideration.

The common theme of the Hall phenomenon was examined by Krishna M. et al. [23] about the successive MHD flow of a water-based nano-stream between two parallel planes. In their study of parabolic flow with MHD, Kavitha et al. [24] looked at the rotational and Dufour effects of uniform temperature and mass diffusion through an accelerating vertical plate while a chemical reaction was taking place. They presented their findings at the end. The effect of Soret and Dufour on MHD flux with heat and mass transfer past a permeable stretching sheet in the presence of thermal radiation was reviewed by Gandluru et al. [25]. They clarified the flux's properties and behaviour. Research on unvarying mass diffusion with thermal radiation and the rotation of a parabolic vertical plate in progress in an MHD setting was investigated by Kathikeyan and Selvaraj [26]. Based on the outcomes, they came to their conclusions. Based on their individual values, Dilip and Selvaraj [27] separately examined the effects of rotation on convective heat and mass transfer on parabolic flux past an accelerated isothermal vertical panel in the presence of a first-order chemical reaction. The stability of bonds, kinetic stability, energy parameters, spectral characterization, GC-MS, and molecular descriptor studies on coumarin have all been explained by Dhanalakshmi et al. [28]. The compounds 3-[2-(1-methyl-2-imidazolylthio)-1-oxoethyl] were employed, such that they shared their insightful findings.

A succinct summary of the applications of TiO_2/jackfruit peel nanocomposites in solar stills: experimental investigation and efficacy evaluation was provided by Alsaiari et al. [29]. Case Studies in Thermal Engineering is where this study is presented. In order to improve the performance of stepped basin solar still natural distillers, Gandhi et al. [30] investigated the synergistic effects of SiO_2/TiO_2 nanolayers in causing thermal absorption and inflammatory reactions in materials. In Sustainable Energy Technologies and Assessments, this study is addressed. Kumar et al. [31] explored the experimental investigation of the performance of a solar still using SiO_2 nanoparticles. The thermal potential of porous materials and the difficulties in enhancing a solar still with TiO_2/jackfruit peel as an improved energy storage material were examined by Asha et al. [32]. They employed particular chemicals to conclude the results. An experimental study on a single-slope, single-basin solar still employing a TiO_2 nanolayer for the creation of natural, clean water was reviewed by Shanmugan et al. [33]. They utilized jackfruit peel or TiO_2 to illustrate how the solar system functions. In order to further increase the productivity of a solar panel, Panchal et al. [34] examined the effects of graphite powder combined with black paint on the absorber panel. In order to enhance the efficiency of a solar desalination unit, Thakur et al. [35] investigated a novel solar absorber that uses activated carbon nanoparticles made from bio-waste. The effect of the MHD stream past an exponentially inclined vertical panel of first-order chemical response with variable mass diffusion and thermal radiation was investigated by Usharani et al. [36]. This study demonstrates that the Dufour and Hall phenomena are both present in MHD flow over a parabolically accelerated vertical plate with uniform temperature and mass diffusion in response to temperature and mass diffusion changes. The study uses Laplace transform techniques to provide numerical solutions to the basic fluid flow equations. Exponential and complementary error function representations will be employed to clarify the mathematical solutions found. Applications in the steel industry, including the ability of hot iron to modulate magnetically during steel production, nuclear reactors for cooling fluid metallic substances, semiconducting materials for hot iron control, meteorology, and other related fields, are strengthened by this kind of research. This study describes the coupled momentum, energy, and concentration fields employing a mathematical model. The governing equations are either numerically or analytically solved, and the outcomes are examined to determine the effects of important parameters like the rotation parameter, Hall parameter, Dufour number, and magnetic field strength. The results shed light on the combined effects of these physical phenomena and lay the groundwork for process optimization in real-world applications.

There are numerous practical applications for the analysis of MHD flow over a parabolically accelerated vertical plate with concentration effects in science and engineering, where it is essential to understand coupled heat and mass transfer under magnetic fields. The ability to regulate solute diffusion directly enhances the quality of the finished product in metallurgical and materials processing processes, such as electromagnetic casting, alloy solidification, and crystal formation. Understanding concentration decay under different Schmidt numbers is crucial for effective cooling and corrosion

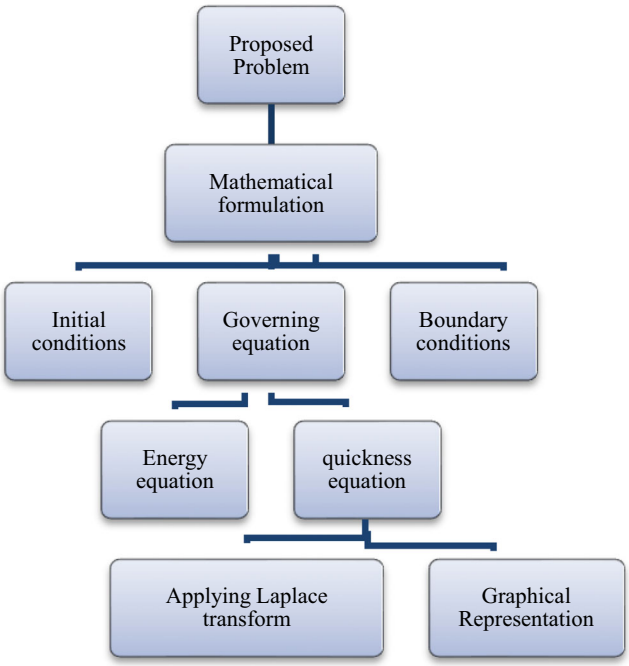

FIGURE 1 Flow chart for the problem.

control in nuclear engineering, especially in liquid metal-cooled reactors. Similar ideas apply to ion diffusion under strong magnetic fields in astronomical and geophysical processes, such as solar winds and stellar atmospheres. Magnetic drug targeting utilizes these transport phenomena in biomedical engineering to maximize drug delivery and particle diffusion. In addition, solute concentration profiles control reaction speeds and efficiency in the chemical and electrochemical industries, including membrane separation, corrosion prevention, and electroplating. Finally, controlling concentration gradients in magnetic environments is essential to environmental and energy systems, including fuel cell technology, hydrogen storage, and pollution dispersion management. Therefore, by demonstrating how concentration changes with time and Schmidt number in MHD flows, the current findings offer important insights for improving these heterogeneous systems [37, 38].

Assumptions of the Problem

1. Over a vertical plate, the flow is laminar, two-dimensional, and unstable.
2. The fluid is electrically conductive, viscous, and incompressible.
3. With time, the vertical plate accelerates parabolically.
4. The induced magnetic field (low magnetic Reynolds number) is ignored when a homogeneous magnetic field is applied normal to the plate.
5. Ion-slip and other higher-order effects are disregarded, although Hall current effects are taken into account.
6. While the Soret effect (mass flux due to temperature gradient) is disregarded, the Dufour effect (energy flux owing to concentration gradient) is included.
7. The system rotates uniformly around a plate-perpendicular axis.
8. The temperature of the plate is consistently higher than that of the fluid.
9. In the fluid medium, variable mass diffusion is taken into account.
10. Except in cases where they manifest as dimensionless quantities, the fluid's physical characteristics, such as its viscosity and thermal conductivity, are taken to be constant.
11. Joule heating and viscous dissipation heat are ignored.
12. The fluid and plate are initially at rest with consistent temperature and concentration.

The flow chart for the considered problem is explained through illustration in Figure 1.

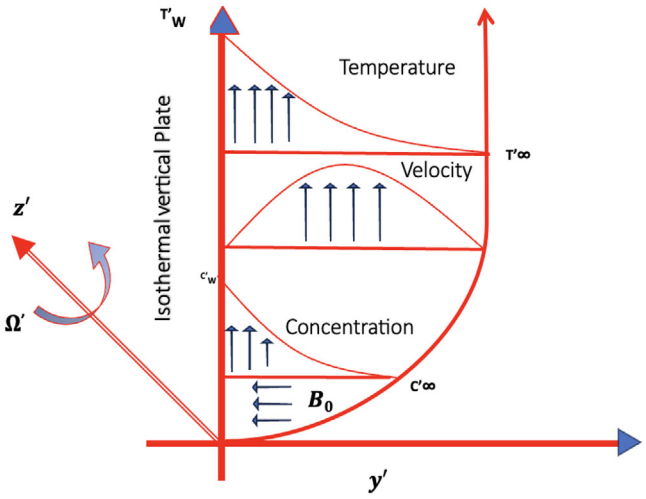

FIGURE 2 Physical model of the problem.

2 | MATHEMATICAL ANALYSIS

The parabolic acceleration of an infinite isothermal plate in the presence of rotation causes a fluid flow in a parabolic pattern outside the plate in the context of 3D-Dufour and Hall effects in MHD. The x'-axis is perpendicular to the direction of irregular flow, the y'-axis parallels the x'-axis, and the Z′-axis is normal to the x'-axis, as depicted in Figure 2. Because of the transverse magnetic field, the fluid and the plate are both rotating steadily around the z-axis at the same angular velocity. It is expected that the viscous dissipation and the precipitated magnetic field will be small. The fluid and the plate were initially both at rest and at the same temperature. Thereafter, the plate was moved perpendicular to its own after $t' > 0$.

When the aforementioned assumptions are considered, the following are the governing equations for momentum, energy, and species concentration in the natural convection flow provided by Soundalgekar [39, 40]

$$\frac{\partial u}{\partial t'} = V\frac{\partial^2 u}{\partial y^2} + 2\Omega' v - \frac{\sigma\,{\mu_e}^2 {B_0}^2}{\rho\,(1+m^2)}(u + mv) + g\beta\left(T' - T'_\infty\right) + g\beta^*\left(C' - C'_\infty\right) \tag{1}$$

$$\frac{\partial v}{\partial t'} = V\frac{\partial^2 v}{\partial y^2} - 2\Omega' u + \frac{\sigma\,{\mu_e}^2 {B_0}^2}{\rho\,(1+m^2)}(mu + v) \tag{2}$$

Energy equation

$$\rho c_p \frac{\partial T'}{\partial t'} = k\frac{\partial^2 T'}{\partial z^2} - \frac{D_m K_T}{C_s C_p}\left(\frac{\partial^2 C'}{\partial {y'}^2}\right) \tag{3}$$

Equation of mass diffusion

$$\frac{\partial C'}{\partial t'} = D\frac{\partial^2 C'}{\partial z^2} \tag{4}$$

where u is the axial velocity and v is the transverse velocity. The prescribed initial and boundary conditions are

$$\left.\begin{array}{c} t' \le 0 \ : u = 0\,, v = 0\,, T' = T'_\infty\,, C' = C'_\infty \ \text{for all } z \\ t' > 0 \ : u = u_0 {t'}^2\,, v = 0\,, T' = T'_\infty + (T_w{}' - T'_\infty)At', C' = C'_\infty + (C_w{}' - C'_\infty)At' \ \text{at } z = 0 \\ t' > 0 \ : u \to 0\,, v \to 0\,, T'.T_\infty{}'\,,\ C'.C_\infty{}' \ \text{as } z \to \infty \end{array}\right\} \tag{5}$$

Considering the dimensionless values shown below

$$\left.\begin{gathered} Z=\frac{yu_0}{\vartheta},\ \bar{t}=\frac{t{u_0}^2}{\vartheta},\ U=\frac{u}{u_0},\ V=\frac{v}{u_0},\theta=\frac{T'-T'_\infty}{T'_w-T'_\infty} \\ \bar{C}=\frac{C'-C'_\infty}{C'_w-C'_\infty}, Gm=\frac{g\beta^*\vartheta\left(C'_w-C_{'\infty}\right)}{{u_0}^3}, r=\frac{g\beta\vartheta\left(T'_w-T'_\infty\right)}{{u_0}^3} \\ M=\frac{\sigma\mu^2{B_0}^2\vartheta}{\rho{u_0}^2\left(1+m^2\right)}, \mathrm{Pr}=\frac{\mu Cp}{k},\ \mu=\vartheta\rho, \bar{\omega}=\frac{\omega\vartheta}{{u_0}^2}, \\ Df=\frac{DmK_T\left(C_w-C_\infty\right)}{\vartheta CsCp\left(T_w-T_\infty\right)} \end{gathered}\right\} \tag{6}$$

Equations (1)–(4) are modified into a non-dimensional form using Equation (6). Below are the dimensionless governing equations that resulted [41].

$$\frac{\partial \mathrm{U}}{\partial \mathrm{t}}=\frac{\partial^2 \mathrm{U}}{\partial \mathrm{Z}^2}+2\Omega \mathrm{V}-\frac{2\mathrm{M}^2}{1+\mathrm{m}^2}(\mathrm{U}-\mathrm{mV})+\mathrm{G_r}\theta+\mathrm{G_m}\mathrm{C} \tag{6}$$

$$\frac{\partial \mathrm{V}}{\partial \mathrm{t}}=\frac{\partial^2 \mathrm{U}}{\partial \mathrm{Z}^2}-2\Omega \mathrm{U}+\frac{2\mathrm{M}^2}{1+\mathrm{m}^2}(\mathrm{mU}-\mathrm{V}) \tag{7}$$

$$\frac{\partial \theta}{\partial \mathrm{t}}=\frac{1}{\mathrm{Pr}}\frac{\partial^2 \theta}{\partial \mathrm{z}^2}-Df\frac{\partial^2 C}{\partial z^2} \tag{8}$$

$$\frac{\partial \mathrm{C}}{\partial \mathrm{t}}=\frac{1}{\mathrm{Sc}}\frac{\partial^2 \mathrm{C}}{\partial \mathrm{z}^2} \tag{9}$$

Removing the bars from Equations (6) to (9) and solving Equations (6) and (7) by adding them together, then applying the complex velocity q = U + iV, results in the combined as single equations represented as (12)

$$\frac{\partial q}{\partial t}=\frac{\partial^2 q}{\partial z^2}+Gr\theta+GmC-aq \tag{10}$$

here a $=\frac{2m^2}{1+m^2}+2i[\Omega-\frac{M^2m}{1+m^2}]$.

Initial and boundary conditions for non-dimensional quantities are

$$\left.\begin{gathered} q=0;\ \theta=0;\ C=0 \quad \forall\, z\ :\ t\le 0 \\ q=\mathrm{t}^2;\ \theta=1;\ C=t \quad \text{at } z=0\ :\ t>0 \\ q\to 0;\ \theta\to 0;\ C\to 0 \quad \text{as } z\to\infty \end{gathered}\right\}. \tag{11}$$

3 | RESULTS AND DISCUSSION

The dimensionless governing Equations (8)–(10), as well as the initial and boundary conditions (13), are solved by applying the Laplace transform method. The corresponding solutions are as follows: Equations (12)–(14) describe the concentration, temperature, and velocity profiles [42].

$$C = t\left[\left(1+2\eta^2 sc\right) erfc\left(\eta\sqrt{sc}\right) - \frac{2\eta\sqrt{sc}}{\sqrt{\pi}} e^{-\eta^2 sc}\right] \tag{12}$$

$$\theta = \left[\frac{Df.pr.sc}{sc-pr}\right]\left\{t\left[\begin{array}{l}\left(\left(1+2\eta^2 pr\right) erfc\left(\eta\sqrt{pr}\right) - \frac{2\eta\sqrt{sc}}{\sqrt{\pi}} e^{-\eta^2 pr}\right) \\ -\left(1+2\eta^2 sc\right) erfc\left(\eta\sqrt{sc}\right) - \frac{2\eta\sqrt{sc}}{\sqrt{\pi}} e^{-\eta^2 sc}\end{array}\right]\right\} + erfc\left(\eta\sqrt{pr}\right) \tag{13}$$

$$q = q_1 + q_2 + q_3 + q_4 + q_5 + q_6. \tag{14}$$

Wherein,

$$q_1 = \frac{1}{2}\left[\frac{\eta^2}{a} + t^2\right]\left[\begin{array}{l}\left[e^{2\eta\sqrt{at}} erfc\left(\eta+\sqrt{at}\right)\right. \\ \left.+e^{-2\eta\sqrt{at}} erfc\left(\eta-\sqrt{at}\right)\right]\end{array}\right]$$

$$q_2 = \left[\left(\frac{1}{4a}-1\right)\left(\frac{\eta\sqrt{t}}{2\sqrt{a}}\right)\right]\left[\begin{array}{l}e^{-2\eta\sqrt{at}} erfc\left(\eta-\sqrt{at}\right) \\ -e^{2\eta\sqrt{at}} erfc\left(\eta+\sqrt{at}\right)\end{array}\right] - \frac{\eta t}{2a\sqrt{\pi}} e^{-\eta^2-at}$$

$$q_3 = \frac{Gr}{pr-1}\left[erfc\left(\eta\sqrt{pr}\right) - \frac{1}{2}\left\{\begin{array}{l}e^{-2\eta\sqrt{at}} erfc\left(\eta-\sqrt{at}\right) \\ -e^{2\eta\sqrt{at}} erfc\left(\eta+\sqrt{at}\right)\end{array}\right\}\right]$$

$$q_4 = \frac{Gm}{sc-1}\left\{\begin{array}{c}\frac{t}{2}\left[\begin{array}{l}e^{-2\eta\sqrt{at}} erfc\left(\eta-\sqrt{at}\right) \\ +e^{2\eta\sqrt{at}} erfc\left(\eta+\sqrt{at}\right)\end{array}\right] \\ -\frac{\eta\sqrt{t}}{2\sqrt{a}}\left[\begin{array}{l}e^{-2\eta\sqrt{at}} erfc\left(\eta-\sqrt{at}\right) \\ +e^{2\eta\sqrt{at}} erfc\left(\eta+\sqrt{at}\right)\end{array}\right] \\ +t[\left(1+2\eta^2 sc\right) erfc\left(\eta\sqrt{sc}\right) \\ -\frac{2\eta\sqrt{sc}}{\sqrt{\pi}} e^{-\eta^2 sc}\end{array}\right\}$$

$$q_5 = \frac{Df.pr.sc.Gr}{(sc-pr)(pr-1)}\left[\begin{array}{c}\left(\frac{\eta\sqrt{t}}{2b\sqrt{a}}-\frac{1}{2b^2}-\frac{t}{b}\right)\left[\begin{array}{l}[e^{2\eta\sqrt{at}}erfc\left(\eta+\sqrt{at}\right)\\+e^{-2\eta\sqrt{at}}erfc\left(\eta-\sqrt{at}\right)\end{array}\right]\\+\frac{e^{bt}}{2b^2}\left[\begin{array}{l}e^{-2\eta\sqrt{(a+b)t}}erfc\left(\eta-\sqrt{(a+b)t}\right)\\-e^{2\eta\sqrt{(a+b)t}}erfc\left(\eta+\sqrt{(a+b)t}\right)\end{array}\right]\\-\left(\frac{1}{b^2}erfc\left(\eta\sqrt{pr}\right)\right)\\-\frac{t}{b}\left[\left(1+2\eta^2pr\right)erfc\left(\eta\sqrt{pr}\right)-\frac{2\eta\sqrt{pr}}{\sqrt{\pi}}e^{-\eta^2pr}\right]\\+\frac{e^{ct}}{2c^2}\left[\begin{array}{l}[e^{-2\eta\sqrt{scct}}erfc\left(\eta\sqrt{sc}-\sqrt{ct}\right)\\+e^{2\eta\sqrt{scct}}erfc\left(\eta\sqrt{sc}+\sqrt{ct}\right)\end{array}\right]\end{array}\right]$$

$$q_6 = \frac{Df.pr.sc.Gr}{(sc-pr)(sc-1)}\left[\begin{array}{c}\left(\frac{\eta\sqrt{t}}{2c\sqrt{a}}-\frac{1}{2c^2}-\frac{t}{c}\right)\left[\begin{array}{l}[e^{2\eta\sqrt{at}}erfc\left(\eta+\sqrt{at}\right)\\+e^{-2\eta\sqrt{at}}erfc\left(\eta-\sqrt{at}\right)\end{array}\right]\\+\frac{e^{ct}}{2c^2}\left[\begin{array}{l}e^{-2\eta\sqrt{(a+c)t}}erfc\left(\eta-\sqrt{(a+c)t}\right)\\-e^{2\eta\sqrt{(a+c)t}}erfc\left(\eta+\sqrt{(a+c)t}\right)\end{array}\right]\\+\frac{1}{c^2}erfc\left(\eta\sqrt{Sc}\right)-\frac{t}{c}\left[\left(1+2\eta^2sc\right)erfc\left(\eta\sqrt{sc}\right)-\frac{2\eta\sqrt{sc}}{\sqrt{\pi}}e^{-\eta^2sc}\right]\\+\frac{e^{ct}}{2c^2}\left[\begin{array}{l}[e^{-2\eta\sqrt{scct}}erfc\left(\eta\sqrt{sc}-\sqrt{ct}\right)\\+e^{2\eta\sqrt{scct}}erfc\left(\eta\sqrt{sc}+\sqrt{ct}\right)\end{array}\right]\end{array}\right].$$

Calculations are based on the outcomes of the Dufour-Hall effect, uniform temperature, and mass diffusion. Mathematical expressions, such as $M = 1$, Gr = Gm = 2, 2, 5, serve as examples. To illustrate complexities, parameters Pr = 0.71, Df = 0.5, and Sc = 0.16 are frequently employed. MATLAB was utilized to generate 2-D visualizations of speed, temperature, and absorption as depicted in Figures 3–12. Following the calculations, the amalgamation of Dufour and Hall effects in the presence of MHD was identified as a potential research technique for solving flow equations [43].

Figure 3 depicts a temperature curve with different Dufour values, Df = 0.2, 0.4 and 0.5 at $t = 0.2$, Pr = 0.71 and Sc = 2.01. The graph illustrates the significant impact of the Dufour number on the temperature distribution in a system. As the Dufour number increases, the temperature rises due to the enhanced heat transfer caused by the concentration gradient. This study highlights the importance of considering the Dufour number in heat transfer analysis, particularly in systems where the concentration gradient plays a crucial role. The Dufour number is a dimensionless quantity that represents the ratio of the heat flux due to the concentration gradient to the heat flux due to the temperature gradient. In essence, it measures the effect of the concentration gradient on the temperature distribution. Fluid temperature near the plate rises as a result of increased thermal energy transmission caused by an enhanced Dufour effect (higher Df). Temperature fields are greatly impacted by concentration gradients because of this phenomenon, which enhances the coupling between heat and mass transfer. Ignoring this parameter might result in an underestimation of the heat transfer rate in engineering systems where Dufour effects are not negligible (such as in multicomponent gas mixtures, porous

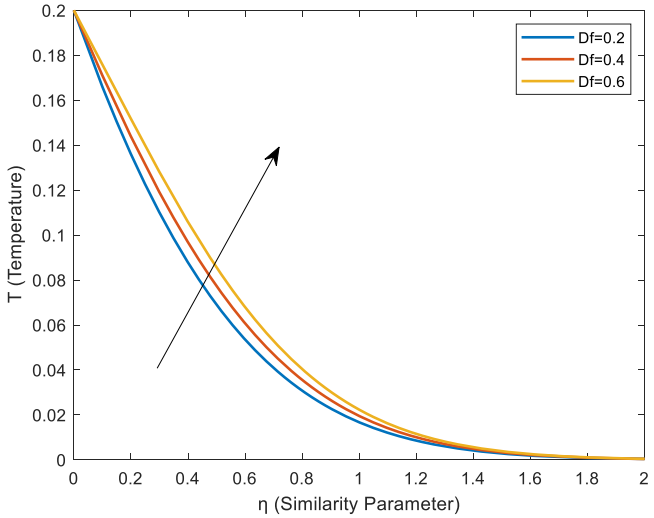

FIGURE 3 Temperature curve for different Df values.

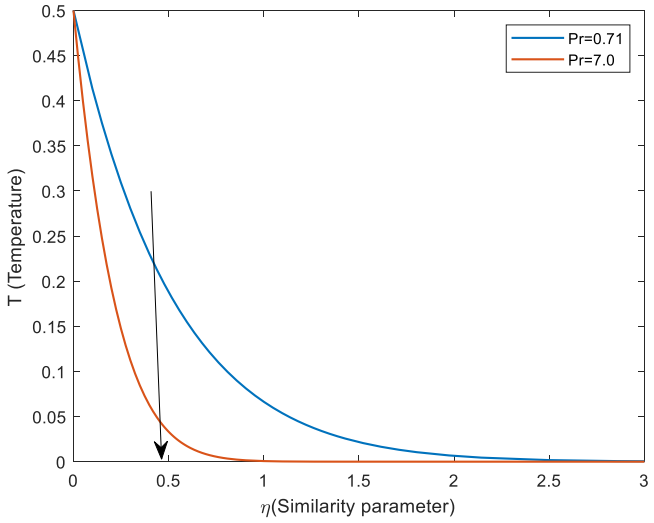

FIGURE 4 Temperature curve for different Pr values.

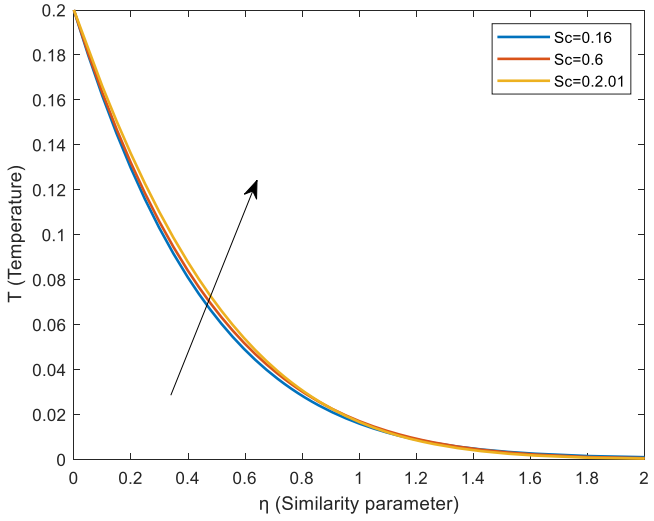

FIGURE 5 Temperature curve for different Sc values.

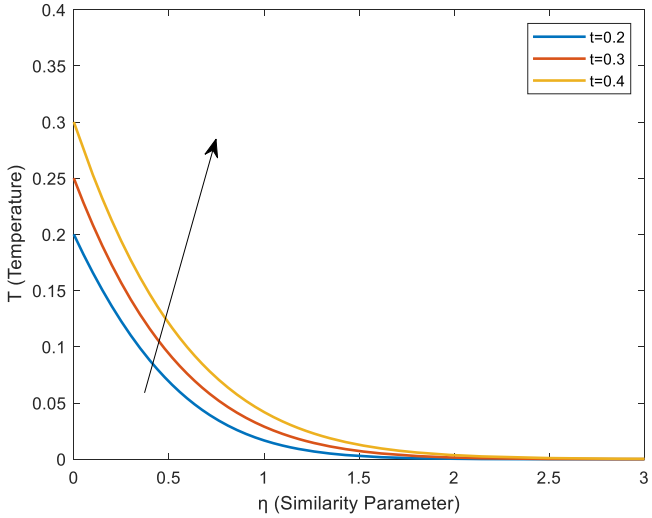

FIGURE 6 Temperature curve for different t values.

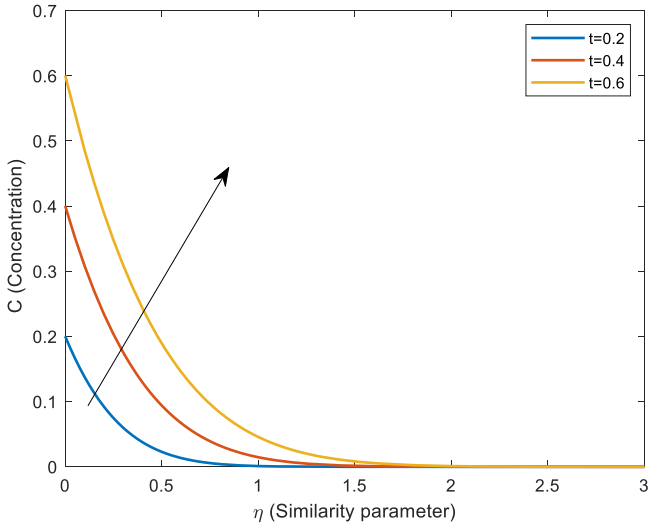

FIGURE 7 Concentration curve for different t values.

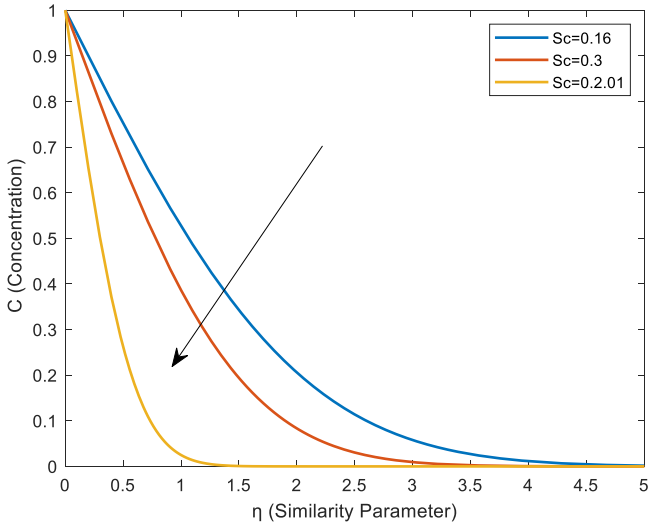

FIGURE 8 Concentration curve for different Sc values.

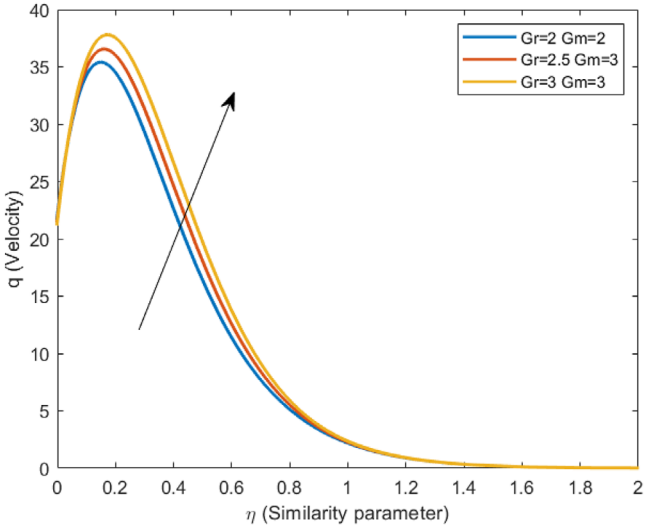

FIGURE 9 Velocity curve for different Gr and Gm values.

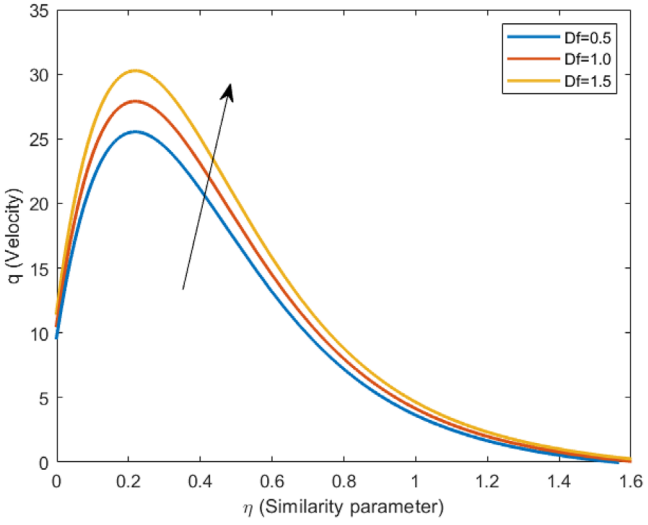

FIGURE 10 Velocity curve for Df values.

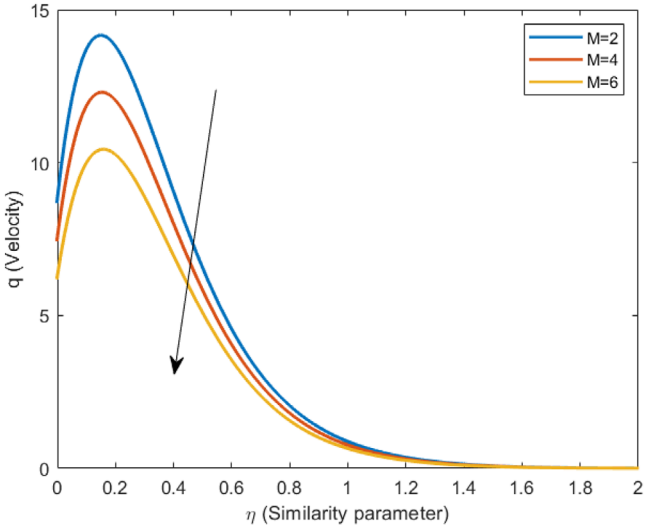

FIGURE 11 Velocity curve for *M* values.

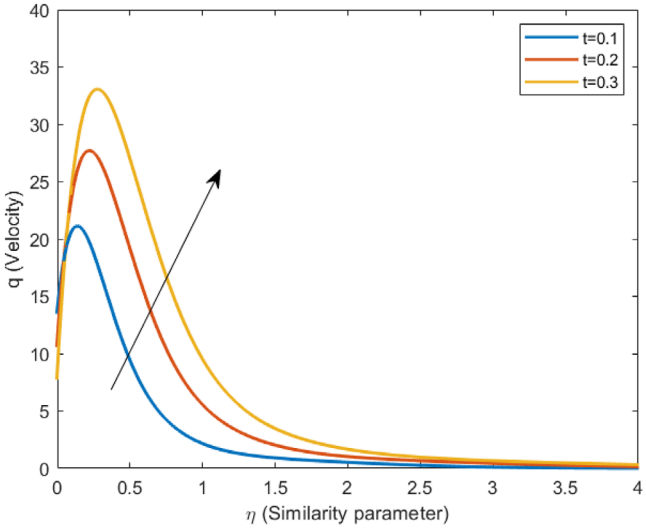

FIGURE 12 Velocity curve for t values.

media, or high-temperature applications). The interaction of magnetic fields, thermal diffusion, and solutal diffusion can significantly alter boundary layer properties for MHD flows in particular, affecting cooling rates, thermal control, and energy efficiency. As a result of thicker thermal boundary layers, the temperature increases as Df increases. In MHD flows over parabolically accelerated vertical plates, heat transport is thus improved by stronger Dufour effects [44].

Figure 4 demonstrates the impacts of the temperature profile for various Prandtl values, especially Pr = 0.71(air) and 7 at $t = 0.2$, Df = 0.2, and Sc = 2.01. The results show that for Pr = 0.71, the temperature is higher than that of Pr = 7, indicating that the air is hotter than the water. As the Prandtl number increases, the temperature drops. The temperature profile drops as Pr values rise from 0.71 to 7. The ratio of momentum diffusivity to thermal diffusivity is represented by the Prandtl number. The thermal diffusivity is greater than the momentum diffusivity when the Prandtl number is smaller (Pr = 0.71). As a result, heat is transferred more effectively, raising the temperature. On the other hand, momentum diffusivity predominates over thermal diffusivity when the Prandtl number is larger (Pr = 7). The temperature drops as a result of less effective heat transfer. The temperature profile changes as a function of Prandtl number, which shows how thermal and momentum diffusivity respond to heat transfer. On the other hand, the thermal boundary layer is significantly thinner for higher Pr values (e.g., Pr = 7.0, corresponding to water) because heat diffusion is less than momentum diffusion, producing steeper temperature gradients close to the plate. This suggests that while fluids with low Pr values permit more thermal penetration into the fluid domain, those with high Pr values cool more quickly and have stronger thermal confinement close to the boundary. Therefore, the result indicates that in MHD flows across accelerated vertical plates, raising Pr decreases the thickness of the thermal boundary layer and increases the rate of heat transfer [45].

Figure 5 depicts the temperature curve for several Schmidt numbers, including Sc = 1.01, 2.01, and 3.01, as well as for t = 0.2, Df = 0.2, and Pr = 0.71. The temperature undergoes a corresponding change as the Schmidt number increases. The Schmidt number represents the ratio of momentum diffusivity to mass diffusivity. A higher Schmidt number indicates a lower mass diffusivity, resulting in a reduced ability to transfer mass. This, in turn, affects the temperature distribution. This suggests that the Schmidt number plays an imperative role in determining the temperature distribution in systems involving mass transfer. The reason for this tendency is that fluids with lower mass diffusivity have greater Schmidt numbers, which strengthens the connection between concentration and thermal diffusion (through the Dufour effect). As a result, heat is held in the fluid farther away from the plate. Conversely, a smaller thermal boundary layer results from stronger mass diffusion at lower Sc, which causes the temperature to decrease more quickly. The result shows that raising the Schmidt number broadens the thermal boundary layer and raises the temperature distribution, indicating the interdependence of mass, heat, and momentum transfer processes in MHD flows across accelerated vertical plates.

Figure 6 displays various temperature profiles for time periods $t = 0.2$, 0.3, and 0.4 with Df = 0.2, Pr = 0.71, and Sc = 2.01. The temperature profiles exhibit significant changes as time progresses. The time-dependent temperature evolution suggests that the system is undergoing a transient heat transfer process. During this process, the temperature distribution changes significantly with time, eventually reaching a steady-state condition. A narrower thermal boundary layer results from the temperature rapidly decaying with the similarity parameter η at earlier times ($t = 0.2$). A thicker thermal bound-

ary layer results from the temperature staying higher for greater distances from the plate as time passes ($t = 0.3$ and $t = 0.4$). This pattern can be explained by the fact that more heat is transported from the plate to the fluid over time, which promotes more thermal diffusion and increased system energy retention. As a result of this behaviour, the thermal field is greatly influenced by the flow's unsteadiness; in MHD flows over accelerated vertical plates, the fluid absorbs more heat energy over time, improving temperature distribution and expanding the thermal boundary layer.

The concentration curves for various time values ($t = 0.2$, 0.4, and 0.6) at a given Schmidt number (Sc = 2.01) are shown in Figure 7. The mass transfer process over time is depicted by the concentration profiles. The concentration at the wall intensifies as time goes on because the concentration gradient close to the wall gets more noticeable. The greater spread of species towards the wall over time is the cause of this phenomenon. The concentration near the wall rises as the species diffuses, creating a more noticeable concentration gradient. The concentration rapidly decays with the similarity parameter η at earlier times ($t = 0.2$), revealing a thin solutal border layer. The concentration stays higher for longer distances from the plate as time passes ($t = 0.4$ and $t = 0.6$), suggesting increased solutal diffusion into the fluid domain. This trend is explained by the cumulative effect of mass transfer over time, which causes the concentration boundary layer to widen as the fluid absorbs more species from the surface over time. The result shows that the solutal transport is significantly governed by the flow's unsteadiness; as time increases, the concentration field becomes stronger, which improves solute penetration and diffusion in MHD flows across accelerated vertical plates.

The concentration curves for different Schmidt numbers (Sc = 0.16, 0.3, and 2.01) at time $t = 0.2$ are shown in Figure 8. The wall concentration drops in tandem with the Schmidt number. The Schmidt number mostly determines the concentration profile. In contrast to Newtonian viscosity, a higher mass diffusivity is indicated by a lower Schmidt number. As a result, species diffuse more effectively, which lowers the concentration of walls. Moreover, a greater Schmidt number indicates a lower mass diffusivity, which makes species diffusion less effective, resulting in the wall concentration rising. It is clear that the concentration boundary layer thickness drastically reduces when the Schmidt number rises from Sc = 0.16 to Sc = 2.01. Fluids with lower mass diffusivity, represented by higher values of Sc, inhibit molecular diffusion and speed up the decay of concentration with respect to the similarity parameter η. On the other hand, because of increased mass diffusivity, the concentration reaches further into the boundary layer region with lower Schmidt numbers. The result shows that species with higher diffusivity (lower Sc) spread farther into the fluid domain, whereas species with smaller molecular diffusivity (higher Sc) are contained closer to the plate surface. This outcome is in line with physics predictions and shows how important the Schmidt number is in controlling the mass transfer properties of magnetohydrodynamic boundary layer flows.

Figure 9 depicts the velocity profiles for different thermal Grashof numbers (Gr = 2, 2.5, and 3) and mass Grashof numbers (Gc = 2, 2, and 3) at $t = 0.2$, Df = 1, Pr = 0.71, Sc = 0.16, $M = 1$, and $m = 1$. Thermal Grashof number influence as the velocity increases, the thermal Grashof number (Gr) rises significantly. The thermal Grashof number expresses the ratio of buoyant forces to viscous forces. As velocity increases, buoyancy forces take precedence, resulting in an increase in the thermal Grashof number. This, in turn, improves the heat transfer process. The association between velocity and thermal Grashof number shows that as fluid velocity increases, so does the thermal Grashof number, resulting in a more pronounced buoyancy effect and improved heat transfer. Overall, the velocity profiles signify a considerable influence on the thermal Grashof number with respect to heat transfer, such that an increase in velocity leads to a considerable increase in the thermal Grashof number, which results in greater heat transfer.

Figure 10 shows velocity profiles for different Dufour numbers (Df = 0.1, 0.2, and 0.3) with fixed parameters $t = 0.2$, m = 1, Pr = 0.71, Sc = 2.01, Gr = 2, Gm = 2, and $M = 2$. The Dufour number has little effect on the velocity profile; a higher Dufour number suggests a stronger influence of the concentration gradient on the heat transfer process. However, in this case, the small gain in velocity despite a significant increase in the Dufour number indicates that the concentration gradient has little effect on the velocity profile. This could be due to the dominance of alternative transport mechanisms, such as thermal diffusion or viscous forces, which outweigh the influence of the Dufour number. In an overall perspective, the velocity profiles reflect that the Dufour number does not have a notable effect on the velocity profile, which implies that alternative transport processes govern the behavior of the flow.

At constant parameters Df = 1.5, t = 0.2, $m = 3$, Pr = 0.71, Sc = 0.16, Gr = 10, and Gm = 50, the velocity profiles for different magnetic parameters ($M = 2$, 4, and 6) are shown in Figure 11. The magnetic parameter (M) rises in proportion to the increase in the magnetic field component. The concomitant rise in M suggests that the flow behaviour is significantly influenced by the magnetic field. Because the magnetic field resists the fluid's motion, the higher magnetic forces may cause the velocity to drop. In the overall analysis, the velocity profiles could clearly indicate how the magnetic parameter extensively affects flow behavior, thereby causing an increase in the magnetic field component, resulting in the magnetic parameter rising in tandem, such that the velocity profile is changed.

TABLE 1 Comparative study with existing literature works.

Reference	Scientific domain	Key contribution	Significance (compared to present work)
Jothi and Selvaraj [3]	MHD, heat transfer	Investigated the heat source impact on MHD fluid flow past an exponentially accelerated plate with radiation absorption through porous media.	Comparison: Addresses radiation absorption, similar to the current study in terms of MHD, but lacks rotation and Hall/Dufour effects.
Sindhu et al. [4]	Parabolic flow, MHD	Analyzed rotational effects on parabolic flow past an isothermal vertical plate with variable temperature and mass diffusion.	Directly relevant as it studies rotational impacts, parabolic flow, and mass diffusion, providing a foundation for the current work.
Gowri and Selvaraj [5]	Fluid dynamics, MHD	Explored unsteady MHD parabolic flow past a vertical plate under rotation in a porous medium.	Comparison: Similar focus on unsteady MHD parabolic flow and rotation, but without Dufour effects.
Dilipjose and Selvaraj [6]	Heat transfer, MHD	Studied heat and mass diffusion in parabolic flow past a vertical plate in the presence of rotation.	Directly related, as it explores both parabolic flow and rotation, essential for the present work, but without Hall/Dufour effects.
Lakshmikanthan et al. [9]	Heat source, MHD	Examined Hall and heat source effects on flow past a parabolically accelerated plate with chemical reaction and radiation.	Crucial comparison with Hall and heat source effects, providing insights into the Hall phenomenon in parabolic flow, like the present study.
Jothi and Selvaraj [10]	MHD, Dufour effect	Investigated the Dufour effect on MHD flow past an exponentially accelerated plate through porous medium with variable temperature.	Directly related to Dufour effect in MHD flow, offering foundational insights for comparison with the present study.
Armstrong et al. [20]	Parabolic flow, rotation	Studied rotational effects on parabolic flow past a vertical plate through porous medium with variable temperature and mass diffusion.	Strong comparison point as it focuses on both rotational effects and parabolic flow, similar to the present research.
Verma and Sharma [18]	MHD, Soret/Dufour effects	Explored Soret and Dufour effects on MHD flow with heat and mass transfer past a stretching sheet.	Relevant as it provides insights into both Dufour and Soret effects, key to understanding the behavior of flows in the present study.
Kavitha et al. [24]	MHD, Dufour effect	Analyzed the Dufour and rotational effects on MHD flow through an accelerating vertical plate with chemical reaction.	Offers direct comparison on Dufour effects combined with rotation, aligning with the present work's objectives.
Dilip Jose and Selvaraj [27]	Heat transfer, MHD	Investigated convective heat and mass transfer effects of rotation on parabolic flow past an isothermal vertical plate with chemical reaction.	Provides insights on rotation and heat/mass transfer effects, crucial for understanding rotational dynamics in the current study.

Figure 12 displays velocity profiles at different time points (t = 0.1, 0.2, and 0.3) with fixed parameters m = 3, M = 2, Pr = 0.71, Sc = 0.16, and Df = 1.5. The decrease in fluid velocity with time can be attributed to higher viscous forces in the fluid. As time passes, the fluid's kinetic energy dissipates due to the action of viscous forces, resulting in a decrease in velocity. Furthermore, the temporal evolution of the velocity profile indicates that the flow is changing from a transient to a steady-state regime. The velocity profile grows more stable over time, indicating that the fluid's velocity changes are less frequent. In generalisation, the velocity profiles could reflect the temporal history of the velocity of fluid, which decreases over time because of the development of increased viscous forces and the transition to a steady-state of the existing flow regime. A comparative study with existing literature works is listed in Table 1.

4 | CONCLUSION

1. This research work provides an analytical solution illustrating the combined effects of Dufour and Hall on magnetohydrodynamic flow across a vertically parabolically accelerated plate with variable mass diffusion and uniform temperature.
2. With the utilization of MATLAB, governing equations were developed that incorporate physical parameters such as Hall and DuFour Effects, Schmidt number, rotational parameters, temperature, and mass Grashof numbers, and time using the Laplace transform method.
3. The presented concise solutions make use of Dufour and Hall effects, among other factors, to assess temperature, concentration, and velocity potentials.
4. Increases in time, Schmidt value, and mass Grashof value cause a corresponding increase in velocity, which decreases as the Dufour value and Hall parameter rise.
5. An increase in time-dependent temperature leads to an increase in the Dufour coefficient. Concentration shows an upward trend over time because a decrease in the Schmidt number is linked to an increase in concentration.
6. The comprehensive analysis of this study has significant implications for materials science, environmental engineering, energy, and aeronautical engineering.
7. With implications for engineering and industrial operations using electrically conducting fluids, these findings offer a greater understanding of the interaction between thermal, mass diffusion, and electromagnetic effects in MHD flows.

NOMENCLATURE

C^*	Species Concentration in the fluid → kg/m^3
C	dimensionless concentration → (unitless)
C_w^*	wall concentration → kg/m^3
C_∞	concentration far away from the Plate → kg/m^3
Cp	specific Heat at Constant Pressure → J/(kg·K)
D	mass diffusion coefficient → m^2/s
Gc	mass Grashof number → (unitless)
Gr	thermal Grashof number → (unitless)
g	accelerated due to gravity → m/s^2
Pr	Prandtl number → (unitless)
Sc	Schmidt number → (unitless)
T	temperature of the fluid near the plate → K
Tw	temperature of the plate → K
$T\infty$	temperature of the fluid far away from the plate → K
t^*	Time → s
t	dimensionless time → (unitless)
u	velocity of the fluid in x-direction → m/s
U_0	velocity of the plate → m/s
q	dimensionless velocity → (unitless)
x	spatial coordinate along the plate → m
y	coordinate axis normal to the plate → m
z	dimensionless coordinate axis normal to the plate →(unitless)
β	volumetric coefficient of thermal expansion →1/k
β^*	volumetric coefficient of thermal expansion
θ	dimensionless temperature → (unitless)
ρ	density of the fluid → kg/m^3
υ	kinematic viscosity → m^2/s
μ	coefficient of viscosity. → Pa·s = kg/(m·s)
η	similarity parameter to (unitless)
$erfc$	complementary error function → (unitless)

Df Dufour number → (unitless)
Ω angular velocity- rad/s

ACKNOWLEDGMENTS
The authors have nothing to report.

CONFLICT OF INTEREST STATEMENT
The authors declare no conflicts of interest.

DATA AVAILABILITY STATEMENT
The data that support the findings of this study are available from the corresponding author upon reasonable request.

ORCID
S. Sahaya Jude Dhas https://orcid.org/0000-0002-2014-0268

REFERENCES
[1] Krishna, M.V., Swarnalathamma, B.V., Chamkha, A.J.: Heat and mass transfer on magnetohydrodynamic chemically reacting flow of a micropolar fluid through a porous medium with Hall effects. Spec. Top. Rev. Porous Media Int. J. 9(4), 347–364 (2018). https://doi.org/10.1615/specialtopicsrevporousmedia.2018024579
[2] Krishna, M.V., Chamkha, A.J.: Hall and ion slip effects on MHD rotating boundary layer flow of nanofluid past an infinite vertical plate embedded in a porous medium. Results Phys. 15, 102652 (2019). https://doi.org/10.1016/j.rinp.2019.102652
[3] Selvaraj, A., Jothi, E.: Heat source impact on MHD and radiation absorption fluid flow past an exponentially accelerated vertical plate with exponentially variable temperature and mass diffusion through a porous medium. Mater. Today: Proc. 46, 3490–3494 (2021). https://doi.org/10.1016/j.matpr.2020.11.919
[4] Sindhu, A., Selvaraj, A., Jose, S.D.: Analysis on rotational impacts of parabolic flow past an accelerated isothermal vertical plate with variable temperature and uniform mass diffusion. Adv. Appl. Math. Sci. 21(11), 6373–6384 (2022)
[5] Gowri, T., Selvaraj, A.: Fluid performance of unsteady MHD parabolic flow past an accelerated vertical plate in the presence of rotation through porous medium. Int. J. Mech. Eng. 7(5), 152–159 (2022)
[6] Selvaraj, A., Jose, S.D., Muthucumaraswamy, R., Karthikeyan, S.: MHD-parabolic flow past an accelerated isothermal vertical plate with heat and mass diffusion in the presence of rotation. Mater. Today: Proc. 46, 3546–3549 (2021). https://doi.org/10.1016/j.matpr.2020.12.499
[7] Jothi, E., Selvaraj, A., Dilipjose, S., Neel Armstrong, A., Karthikeyan, S.: Effect of MHD and Radiation Absorption Fluid Flow Past an Exponentially Accelerated Vertical Plate with Variable Temperature and Concentration. In *Proceedings of the First International Conference on Mathematical Modeling and Computational Science*, pp. 429–439 (2021) https://doi.org/10.1007/978-981-33-4389-4_39
[8] Aruna, M., Selvaraj, A., Rekha, V.: Hall and Magnetic Impacts on Stream Past a Parabolic Accelerated Vertical Plate with Varying Heat and Uniform Mass Diffusion in the Appearance of Thermal Radiation. *Recent Advances in Intelligent Manufacturing. Select Proceedings of ICAME*, pp. 323–336 (2023). https://doi.org/10.1007/978-981-99-1308-4_26
[9] Lakshmikaanth, D., Selvaraj, A., Selvaraju, P., Jose, S.D.: Hall and heat source effects of flow past a parabolic accelerated isothermal vertical plate in the presence of chemical reaction and radiation. JP J. Heat Mass Transf. 34, 105–126 (2023). https://doi.org/10.17654/0973576323035
[10] Jothi, E., Selvaraj, A.: Dufour effect on MHD flow past an exponentially accelerated vertical plate through a porous system with variable temperature and mass diffusion. J. Math. Comput. Sci. 11(5), 6205–6215 (2021). https://doi.org/10.17654/0973576323035
[11] Lakshmikanthan, D., Selvaraj, A., Neel Armstrong, A.: Heat Source effects of flow past a parabolic accelerated isothermal vertical plate in the presence of Hall Current, Chemical reaction, Rotation and Radiation. Eur. Chem. Bul. 2(4), 6205–6215 (2023)
[12] Jothi, E., Selvaraj, A.: Performance of Dufour effect on unsteady MHD flow past through porous medium an exponentially accelerated inclined vertical plate with variable temperature and mass diffusion. Turk. J. Comput. Math. Educ. 12(12), 3457–3463 (2021). https://doi.org/10.17762/turcomat.v12i12.8070
[13] Angela, S.C., Selvaraj, A.: Dufour and hall effects on MHD flow past an exponentially accelerated vertical plate with variable temperature and mass diffusion. Turk. J. Comput. Math. Educ. 12(6), 3542–3556 (2021). https://doi.org/10.17762/turcomat.v12i6.7143
[14] Turkyilmazoglu, M.: Effects of uniform radial electric field on the MHD heat and fluid flow due to a rotating disk. Int. J. Eng. Sci. 51, 233–240 (2012). https://doi.org/10.1016/j.ijengsci.2011.09.011
[15] Priyadarshini, S.I., Armstrong, A.N.: Skin friction analysis of parabolic started infinite vertical plate with variable temperature and variable mass diffusion in the presence of a magnetic field. Int. J. Pure Appl. Math. 116(24), 89–92 (2017)
[16] Reddy, A.D., Reddy, P., Kuntumalla, B.L., Madhura, S.L., Areti, P.: Heat and mass transfer flow on magneto hydro dynamic convective flow through Porous medium between Infinite vertical plate with Soret and Joules dissipation. Tuijin Jishu/J. Propuls. Technol. 44(4), 5114–5124 (2023)
[17] Karim, M.E., Samad, M.A., Hasan, M.M.: Dufour and Soret effect on steady MHD flow in the presence of Heat generation and magnetic field past an inclined stretching sheet. Open J. Fluid Dyn. 2(3), 91–100 (2012). http://doi.org/10.4236/ojfd.2012.23009

[18] Verma, K., Sharma, B.R.: Soret and Dufour effects on MHD flow with heat and mass transfer past an exponentially stretching sheet. Lat. Am. Appl. Res. Int. J. 52(2), 83–88 (2022). https://doi.org/10.52292/j.laar.2022.795
[19] Ercan, N.U.: Hall impact on the MHD fluid flow and heat transfer with uniform radial electric field due to a stretching rotating disk. Hacet. J. Math. Stat. 51(2), 509–524 (2022). https://doi.org/10.15672/hujms.735733
[20] Armstrong, A.N., Dhanasekar, N., Selvaraj, A., Shanmugapriya, R., Hemalatha, P.K., Kumar, J.N.: Rotational effect of parabolic flow past in a vertical plate through porous medium with variable temperature and uniform mass diffusion. In *AIP Conference Proceedings*, vol. 282191, 080016 (2023). https://doi.org/10.1063/5.0158630
[21] Seth, G.S., Kumbhakar, B., Sharma, R.: Unsteady MHD free convection flow with Hall effect of a radiating and heat absorbing fluid past a moving vertical plate with variable ramped temperature. J. Egyptian Math. Soc. 24(3), 471–478 (2016). https://doi.org/10.1016/j.joems.2015.07.007
[22] Muthucumaraswamy, R., Prema, K.M.A.: Hall effect on moving isothermal vertical plate with variable temperature and mass diffusion in the presence of rotating fluid. Int. J. Adv. Sci. Technol. Eng. Manag. Sci. 2(8), 6–13 (2016). http://doi.org/10.13140/RG.2.2.33144.49927
[23] Krishna, M.V., Chamkha, A.J.: Hall effects on MHD squeezing flow of a water-based nanofluid between two parallel disks. J. Porous Media 22(2), 209–223 (2019). http://doi.org/10.1615/JPorMedia.2018028721
[24] Kavitha, S., Selvaraj, A., Senthamilselvi, S., Rajesh, P.: A parabolic flow with MHD, the dufour and rotational effects of uniform temperature and mass diffusion through an accelerating vertical plate in the presence of chemical reaction. J. Adv. Res. Fluid Mech. Therm. Sci. 110(2), 192–205 (2023). https://doi.org/10.37934/arfmts.110.2.192205
[25] Sreedevi, G., Prasada Rao, D.R.V., Makinde, O.D., Venkata Ramana Reddy, G.: Soret and Dufour effects on MHD flow with heat and mass transfer past a permeable stretching sheet in presence of thermal radiation. Indian J. Pure Appl. Phys. 55(8), 551–563 (2017). http://op.niscair.res.in/index.php/IJPAP/article/view/13883/0
[26] Karthikeyan, S., Selvaraj, A.: Uniform mass diffusion on thermal radiation with rotation of parabolic in progress vertical plate set MHD. Mater. Today: Proc. 51, 1074–1078 (2022). http://doi.org/10.1016/j.matpr.2021.07.098
[27] Jose, S.D., Selvaraj, A.: Convective heat and mass transfer effects of rotation on parabolic flow past an accelerated isothermal vertical plate in the presence of chemical reaction of first order. JP J. Heat Mass Transf. 24(1), 191–206 (2021). https://doi.org/10.17654/HM024010191
[28] Dhanalakshmi, E., Rajesh, P., Kandan, P., Kesavan, M., Jayaraman, G., Selvaraj, A., Priya, R.: Stability of bonds, kinetic stability, energy parameters, spectral characterization, GC–MS and molecular descriptors studies on coumarine, 3-[2-(1-methyl-2-imidazolylthio)-1-oxoethyl]. J. Mol. Struct. 1295, 136544 (2024). https://doi.org/10.1016/j.molstruc.2023.136544
[29] Alsaiari, A.O., Shanmugan, S., Abulkhair, H., Bamasag, A., Moustafa, E.B., Alsulami, R.A., Elsheikh, A.: Applications of TiO_2/Jackfruit peel nanocomposites in solar still: Experimental analysis and performance evaluation. Case Stud. Therm. Eng. 38, 102292 (2022) https://doi.org/10.1016/j.csite.2022.102292
[30] Gandhi, A.M., Shanmugan, S., Kumar, R., Elsheikh, A.H., Sharifpur, M., Bewoor, A.K., Ongar, B.: SiO_2/TiO_2 nanolayer synergistically triggers thermal absorption inflammatory responses, materials for performance improvement of stepped basin solar still natural distiller. Sustain. Energy Technol. Assess. 52, 101974 (2022). https://doi.org/10.1016/j.seta.2022.101974
[31] Kumar, T.R., Shanmugan, S., Sundari, G.S., Devi, N.P.L., Abhiram, N., Palanikumar, G.: Experimental investigation on the performance of a solar still using SiO_2 nanoparticles/Jatropha curcas L. Silicon 14(7), 3501–3514 (2022). https://doi.org/10.1007/s12633-021-01119-y
[32] Asha, S., Shanmugan, S., Venkateswarlu, M., Meenachi, M., Sangeetha, A., Rao, M.C.: Thermal potential porous materials and challenges of improving solar still using TiO_2/Jackfruit peel-enhanced energy storage material. Mater. Today: Proc. 66, 3616–3625 (2022). https://doi.org/10.1016/j.matpr.2022.07.142
[33] Shanmugan, S., Essa, F.A., Gorjian, S., Kabeel, A.E., Sathyamurthy, R., Manokar, A.M.: Experimental study on single slope single basin solar still using TiO_2 nano layer for natural clean water invention. J. Energy Storage 30, 101522 (2020). https://doi.org/10.1016/j.est.2020.101522
[34] Panchal, H., Sadasivuni, K.K., Ahmed, A.A.A., Hishan, S.S., Doranehgard, M.H., Essa, F.A., … Khalid, M.: Graphite powder mixed with black paint on the absorber plate of the solar still to enhance yield: An experimental investigation. Desalination 520, 115349 (2021). https://doi.org/10.1016/j.desal.2021.115349
[35] Thakur, A.K., Sathyamurthy, R., Velraj, R., Saidur, R., Lynch, I., Venkatesh, R., Sillanpää, M.: A novel solar absorber using activated carbon nanoparticles synthesized from bio-waste for the performance improvement of solar desalination unit. Desalination 527, 115564 (2022). https://doi.org/10.1016/j.desal.2022.115564
[36] Usharani, V., Selvaraj, A., Constance Angela, R., Neel Armstrong, A.: Impact of MHD stream past an exponentially inclined vertical plate of first-order chemical response with variable mass diffusion and thermal radiation. In *Proceedings of the First International Conference on Mathematical Modeling and Computational Science. ICMMCS 2020*, pp. 485–497 (2021) https://doi.org/10.1007/9
[37] Krishna, M.V., Swarnalathamma, B.V.: Convective heat and mass transfer on MHD peristaltic flow of Williamson fluid with the effect of inclined magnetic field. In *AIP Conference Proceedings* (2016). https://doi.org/10.1063/1.4946512
[38] Krishna, M.V., Chamkha, A.J.: Hall and ion slip effects on MHD rotating flow of elastico-viscous fluid through porous medium. Int. Commun. Heat Mass Transf. 113, 104494 (2020). https://doi.org/10.1016/j.icheatmasstransfer.2020.104494
[39] Soundalgekar, V.M.: Effects of mass transfer and free-convection currents on the flow past an impulsively started vertical plate. J. Appl. Mech. 46(4), 757–760 (1979). http://doi.org/10.1115/1.3424649
[40] Soundalgekar, V.M.: Effects of mass transfer on flow past a uniformly accelerated vertical plate. Lett. Heat Mass Transf. 9(1), 65–72 (1982). https://doi.org/10.1016/0094-4548(82)90049-2

[41] Goud, B.S., Srilatha, P., Mahendar, D., Srinivasulu, T., Reddy, Y.D.: Thermal radiation effect on thermostatically stratified MHD fluid flow through an accelerated vertical porous plate with viscous dissipation impact. Partial Differ. Equ. Appl. Math. 7, 100488 (2023). https://doi.org/10.1016/j.padiff.2023.100488

[42] Krishna, M.V.: Diffusion-thermo, Thermo-diffusion, Hall and ion slip effects on MHD flow through porous medium in a rotating channel. Chem. Phys. 112623 (2025). https://doi.org/10.1016/j.chemphys.2025.112623

[43] Gayathri, M., Babu, B.H., Krishna, M.V.: Soret and Dofour effects on unsteady MHD convection flow over an infinite vertical porous plate. Mod. Phys. Lett. B (2024). https://doi.org/10.1142/s0217984924504499

[44] Ahamad, N.A., Krishna, M.V., Chamkha, A.J.: Radiation-absorption and Dufour effects on magnetohydrodynamic rotating flow of a nanofluid over a semi-infinite vertical moving plate with a constant heat source. J. Nanofluids 9(3), 177–186 (2020). https://doi.org/10.1166/jon.2020.1743

[45] Krishna, M.V.: Numerical investigation on steady natural convective flow past a perpendicular wavy surface with heat absorption/generation. Int. Commun. Heat Mass Transf. 139, 106517 (2022). https://doi.org/10.1016/j.icheatmasstransfer.2022.106517

How to cite this article: Selvaraj, A., Aruna, M., Deepa, S., Dilip Jose, S., Dhas, S.S.J., Alotaibi, M.T.: Harnessing of potential Hall and Dufour Effects on MHD flow over a parabolically accelerated vertical plate. Z Angew Math Mech. 105, e70288 (2025). https://doi.org/10.1002/zamm.70288